

Diffusion in hollow cylinders with mathematical treatment

Ching Chiang Hwang¹, Ing-Bang Huang²

¹Department of Biotechnology, Mingdao University, Taiwan

²Department of Materials Science and Engineering, National Formosa University, Huwei, Yulin, 63201, Taiwan

Abstract—Diffusion-induced stresses in hollow cylinders for decay transient states were investigated. Two cases are considered and studied, the first case is a diffusion process, with the initial concentration described by $C=C_0\ln(r/a)\ln(b/a)$, in which the solute diffuses from outer into inner surfaces when steady state has finished and zero concentrations at both boundary surfaces. The second case, with the initial concentration described by $C=-C_0\ln(r/b)\ln(b/a)$, in which the solute diffuses from inner into outer surfaces when steady state has finished and zero concentrations at both boundary surfaces. The stress formulas in the hollow cylinder were derived. The radial stress, tangential stress, axial stress and the maximum shear stress for zero axial force are calculated.

Keywords—Diffusion-Induced stress; Hollow cylinder; Diffusion; decay transient states

I. INTRODUCTION

Diffusion-induced stresses are built up by composition during mass transfer. According to Prussin [1] and Li [2], the stresses arising from a concentration distribution are similar to the thermal stresses induced by a temperature distribution in an elastic medium. One of the most important effects of diffusion-induced stresses is dislocation generation. This effect improves the mechanical properties of steel [3]. Li, Lee and coworkers [4-7] have made extensive studies on diffusion-induced stresses in various systems including thin slab, long bars and solid cylinder, solid sphere and composites. Recently, Lee et al. [8-9] studied the diffusion-induced stresses in a hollow cylinder for constant surface concentration, constant average concentration and instantaneous surface concentration for one special case. However, the decay part of diffusion-induced stresses has been mostly neglected by the previous workers. A more general mathematical solution of diffusion-induced stresses for decay transient state in hollow cylinders with different outer/inner radius ratio has not been found to our knowledge. In this paper, both the concentration profiles and stress distribution profiles were presented, respectively.

II. CONCENTRATION DISTRIBUTION

Consider an isotropic medium of hollow cylinder with inner radius a and outer radius b . Assume that the diffusion coefficient D is constant. According to Fick's law, the solute concentration C satisfies the diffusion equation in the cylindrical coordinate,

$$\frac{\partial C}{\partial t} = D \left(\frac{\partial^2 C}{\partial r^2} + \frac{1}{r} \frac{\partial C}{\partial r} \right) \quad (1)$$

where r is the radial variable and t is the time in the cylindrical coordinate, respectively.

2.1. Decay transient state

Similar to the solution of the temperature distribution solved by Carslaw and Jaeger [10], both diffusion processes of constant surface concentration source from outer into inner surfaces and reverse case including steady, set up transient, and decay transient states have been studied [11].

2.1.1. Case A

Consider the concentration of the steady state as the initial condition and the boundary conditions on the two surfaces are

$$t \leq 0, a < r < b, C = C_0 \frac{\ln\left(\frac{r}{a}\right)}{\ln\left(\frac{b}{a}\right)} \quad (2)$$

$$t > 0, r = a, C = 0$$

$$t > 0, r = b, C = 0$$

The solution of this case has been derived and discussed in our previous paper [11] and are rewritten as

$$C = \pi C_0 \sum_{n=1}^{\infty} \frac{J_0^2(b\alpha_n)U_0(r\alpha_n)}{J_0^2(a\alpha_n) - J_0^2(b\alpha_n)} \exp(-D\alpha_n^2 t) \quad (3)$$

The normalized concentration of this case can be expressed as

$$\frac{C}{C_0} = \pi \sum_{n=1}^{\infty} \frac{J_0^2(a\alpha_n)U_0(a\alpha_n r^*)}{J_0^2(a\alpha_n) - J_0^2(k\alpha_n)} \exp[-(a\alpha_n)^2 \tau] \quad (4)$$

where

$$U_0(a\alpha_n r^*) = J_0(a\alpha_n r^*)Y_0(k\alpha_n) - Y_0(a\alpha_n r^*)J_0(k\alpha_n)$$

$$r^* = \frac{r}{a} \quad k = \frac{b}{a} \quad \tau = \frac{Dt}{a^2}$$

Where α_n are the positive roots of function $J_0(a\alpha_n)Y_0(b\alpha_n) - J_0(b\alpha_n)Y_0(a\alpha_n)$ as given in Table 1 [10].

Table 1

Roots of $J_0(a\alpha_n)Y_0(b\alpha_n) - J_0(b\alpha_n)Y_0(a\alpha_n)$.

$\frac{b}{a}$	$a\alpha_1$	$a\alpha_2$	$a\alpha_3$	$a\alpha_4$	$a\alpha_5$
1.2	15.7014	31.4126	47.1217	62.8302	78.5385
1.5	6.2702	12.5598	18.8451	25.1294	31.4133
2.0	3.1230	6.2734	9.4182	12.5614	15.7040
2.5	2.0732	4.1773	6.2754	8.3717	10.4672
3.0	1.5485	3.1291	4.7038	6.2767	7.8487
3.5	1.2339	2.5002	3.7608	5.0196	6.2776
4.0	1.0244	2.0809	3.1322	4.1816	5.2301

2.1.2. Case B

Consider the concentration of the steady state as the initial condition and the boundary conditions on the two surfaces are

$$t \leq 0, a < r < b, C = C_0 \frac{\ln\left(\frac{b}{r}\right)}{\ln\left(\frac{b}{a}\right)}$$

$$t > 0, \quad r = a, C = 0$$

$$t > 0, \quad r = b, C = 0$$

(5)

The solution of this case has been derived and discussed earlier [11] and are rewritten as

$$C = -\pi C_0 \sum_{n=1}^{\infty} \frac{J_0(a\alpha_n)J_0(b\alpha_n)U_0(r\alpha_n)}{J_0^2(a\alpha_n) - J_0^2(b\alpha_n)} \exp(-D\alpha_n^2 t) \quad (6)$$

The normalized concentration of this case is

$$\frac{C}{C_0} = -\pi \sum_{n=1}^{\infty} \frac{J_0(a\alpha_n)J_0(k\alpha_n)U_0(k\alpha_n r^{**})}{J_0^2(a\alpha_n) - J_0^2(k\alpha_n)} \exp[-(a\alpha_n)^2 \tau] \quad (7)$$

Where

$$U_0(k\alpha_n r^{**}) = J_0(k\alpha_n r^{**})Y_0(k\alpha_n) - Y_0(k\alpha_n r^{**})J_0(k\alpha_n)$$

$$r^{**} = \frac{r}{b} \quad k = \frac{b}{a} \quad \tau = \frac{Dt}{a^2}$$

2.2 stress distribution

The derivation of stress distribution arising from the solute diffusion is similar to the thermal stresses arising from the heat transfer if the thermal expansion coefficient and temperature are replaced by one-third of the partial molar volume and concentration, respectively [12]. The radial stress, tangential stress and axial stress can be expressed as

$$\sigma_{rr} = \frac{\bar{V}E}{3(1-\nu)r^2} \left(\frac{r^2 - a^2}{b^2 - a^2} \int_a^b C r dr - \int_a^r C r dr \right) \quad (8)$$

$$\sigma_{\theta\theta} = \frac{\bar{V}E}{3(1-\nu)r^2} \left(\frac{r^2 + a^2}{b^2 - a^2} \int_a^b C r dr + \int_a^r C r dr - C r^2 \right) \quad (9)$$

$$\sigma_{zz} = \frac{\bar{V}E}{3(1-\nu)} \left(\frac{2}{b^2 - a^2} \int_a^b C r dr - C \right) \quad (10)$$

2.2.1. Case A

In this case, the following two integrals are used for calculation of stresses,

$$\int_a^r r U_0(r\alpha_n) dr = -\frac{r}{\alpha_n} \{J_0(b\alpha_n)Y_1(r\alpha_n) - Y_0(b\alpha_n)J_1(r\alpha_n)\} - \frac{2J_0(b\alpha_n)}{\pi\alpha_n^2 J_0(a\alpha_n)} \quad (11)$$

$$\int_a^b r U_0(r\alpha_n) dr = \frac{2\{J_0(a\alpha_n) - J_0(b\alpha_n)\}}{\pi\alpha_n^2 J_0(a\alpha_n)} \quad (12)$$

Substituting Eqs. (11)-(12) into Eqs. (8)-(10), one obtains

$$\frac{\sigma_{rr}}{\bar{V}EC_0} = \left\{ \frac{r^{*2} - 1}{k^2 - 1} \sum_{n=1}^{\infty} \frac{2J_0^2(k\alpha_n)}{(a\alpha_n r^*)^2 J_0(a\alpha_n)[J_0(a\alpha_n) + J_0(k\alpha_n)]} + \right.$$

$$\left. \pi \sum_{n=1}^{\infty} \frac{J_0^2(k\alpha_n)[J_0(k\alpha_n)Y_1(a\alpha_n r^*) - Y_0(k\alpha_n)J_1(a\alpha_n r^*)]}{a\alpha_n r^* [J_0^2(a\alpha_n) - J_0^2(k\alpha_n)]} \right\} +$$

$$\sum_{n=1}^{\infty} \frac{2J_0^3(k\alpha_n)}{(a\alpha_n r^*)^2 J_0(a\alpha_n)[J_0^2(a\alpha_n) - J_0^2(k\alpha_n)]} \} \times \exp[-(a\alpha_n)^2 \tau] \quad (13)$$

$$\frac{\sigma_{\theta\theta}}{VEC_0} = \left\{ \frac{r^{*2} + 1}{k^2 - 1} \sum_{n=1}^{\infty} \frac{2J_0^2(k\alpha_n)}{(a\alpha_n r^*)^2 J_0(a\alpha_n)[J_0(a\alpha_n) + J_0(k\alpha_n)]} - \frac{1}{3(1-\nu)} \right.$$

$$\left. \pi \sum_{n=1}^{\infty} \frac{J_0^2(k\alpha_n)[J_0(k\alpha_n)Y_1(a\alpha_n r^*) - Y_0(k\alpha_n)J_1(a\alpha_n r^*)]}{a\alpha_n r^* [J_0^2(a\alpha_n) - J_0^2(k\alpha_n)]} - \frac{2J_0^3(k\alpha_n)}{(a\alpha_n r^*)^2 J_0(a\alpha_n)[J_0^2(a\alpha_n) - J_0^2(k\alpha_n)]} - \pi \sum_{n=1}^{\infty} \frac{J_0^2(k\alpha_n)U_0(a\alpha_n r^*)}{J_0^2(a\alpha_n) - J_0^2(k\alpha_n)} \right\} \times \exp[-(a\alpha_n)^2 \tau] \quad (14)$$

$$\frac{\sigma_{zz}}{VEC_0} = \left\{ \frac{4r^{*2}}{k^2 - 1} \sum_{n=1}^{\infty} \frac{J_0^2(k\alpha_n)}{(a\alpha_n r^*)^2 J_0(a\alpha_n)[J_0(a\alpha_n) + J_0(k\alpha_n)]} - \frac{1}{3(1-\nu)} \right.$$

$$\left. \pi \sum_{n=1}^{\infty} \frac{J_0^2(k\alpha_n)U_0(a\alpha_n r^*)}{J_0^2(a\alpha_n) - J_0^2(k\alpha_n)} \right\} \times \exp[-(a\alpha_n)^2 \tau] \quad (15)$$

where

$$U_0(a\alpha_n r^*) = J_0(a\alpha_n r^*)Y_0(k\alpha_n) - Y_0(a\alpha_n r^*)J_0(k\alpha_n)$$

$$r^* = \frac{r}{a} \quad k = \frac{b}{a} \quad \tau = \frac{Dt}{a^2}$$

2.2.2. Case B

In order to compute the stress distribution, the following two integrations are required.

$$\int_a^r r U_0(r\alpha_n) dr = -\frac{r}{\alpha_n} \{ J_0(b\alpha_n)Y_1(r\alpha_n) - Y_0(b\alpha_n)J_1(r\alpha_n) \} - \frac{2J_0(b\alpha_n)}{\pi\alpha_n^2 J_0(a\alpha_n)} \quad (16)$$

Substituting Eqs. (12)- (16) into Eqs. (8)- (10), one obtains

$$\frac{\sigma_{rr}}{\frac{VEC_0}{3(1-\nu)}} = \left\{ -\frac{(kr^{**})^2 - 1}{k^2 - 1} \sum_{n=1}^{\infty} \frac{2J_0(k\alpha_n)}{(k\alpha_n r^{**})^2 [J_0(\alpha_n) + J_0(k\alpha_n)]} - \right.$$

$$\pi \sum_{n=1}^{\infty} \frac{J_0(\alpha_n) J_0(k\alpha_n) [J_0(k\alpha_n) Y_1(k\alpha_n r^{**}) - Y_0(k\alpha_n) J_1(k\alpha_n r^{**})]}{k\alpha_n r^{**} [J_0^2(\alpha_n) - J_0^2(k\alpha_n)]} -$$

$$\left. \sum_{n=1}^{\infty} \frac{2J_0^2(k\alpha_n)}{(k\alpha_n r^{**})^2 [J_0^2(\alpha_n) - J_0^2(k\alpha_n)]} \right\} \times \exp[-(\alpha_n)^2 \tau] \quad (17)$$

$$\frac{\sigma_{\theta\theta}}{\frac{VEC_0}{3(1-\nu)}} = \left\{ -\frac{(kr^{**})^2 + 1}{k^2 - 1} \sum_{n=1}^{\infty} \frac{2J_0(k\alpha_n)}{(k\alpha_n r^{**})^2 [J_0(\alpha_n) + J_0(k\alpha_n)]} + \right.$$

$$\pi \sum_{n=1}^{\infty} \frac{J_0(\alpha_n) J_0(k\alpha_n) [J_0(k\alpha_n) Y_1(k\alpha_n r^{**}) - Y_0(k\alpha_n) J_1(k\alpha_n r^{**})]}{k\alpha_n r^{**} [J_0^2(\alpha_n) - J_0^2(k\alpha_n)]} +$$

$$\left. \sum_{n=1}^{\infty} \frac{2J_0^2(k\alpha_n)}{(k\alpha_n r^{**})^2 [J_0^2(\alpha_n) - J_0^2(k\alpha_n)]} + \pi \sum_{n=1}^{\infty} \frac{J_0(\alpha_n) J_0(k\alpha_n) U_0(k\alpha_n r^{**})}{J_0^2(\alpha_n) - J_0^2(k\alpha_n)} \right\}$$

$$\times \exp[-(\alpha_n)^2 \tau] \quad (18)$$

$$\frac{\sigma_{zz}}{\frac{VEC_0}{3(1-\nu)}} = \left\{ -\frac{2(kr^{**})^2}{k^2 - 1} \sum_{n=1}^{\infty} \frac{2J_0(k\alpha_n)}{(k\alpha_n r^{**})^2 [J_0(\alpha_n) + J_0(k\alpha_n)]} + \right.$$

$$\left. \pi \sum_{n=1}^{\infty} \frac{J_0(\alpha_n) J_0(k\alpha_n) U_0(k\alpha_n r^{**})}{J_0^2(\alpha_n) - J_0^2(k\alpha_n)} \right\} \times \exp[-(\alpha_n)^2 \tau] \quad (19)$$

Where

$$U_0(k\alpha_n r^{**}) = J_0(k\alpha_n r^{**}) Y_0(k\alpha_n) - J_0(k\alpha_n) Y_0(k\alpha_n r^{**})$$

$$r^{**} = \frac{r}{b} \quad k = \frac{b}{a} \quad \tau = \frac{Dt}{a^2}$$

III. RESULTS AND DISCUSSION

3.1. Radial stresses

For cases A and B, some values of $\sigma_{rr}/[VEC_0/3(1-V)]$ predicted by Eqs. (13) and (17) are plotted against r^* and r^{**} for $k = 1.2, 2$ and 4 , at various time as shown in Figs. 1 (a)-(c) and Figs. 2 (a)-(c), respectively.

As shown in Figs. 1, for case A, the radial stress component σ_r is tensile in the region near the inner surface and compressive near the outer surface. The stress distribution decreases with increasing time. The curves of σ_r are similar to sine curves. Furthermore, for case B, the radial stress has the same situation as that in case A as shown in the Figs. 2.

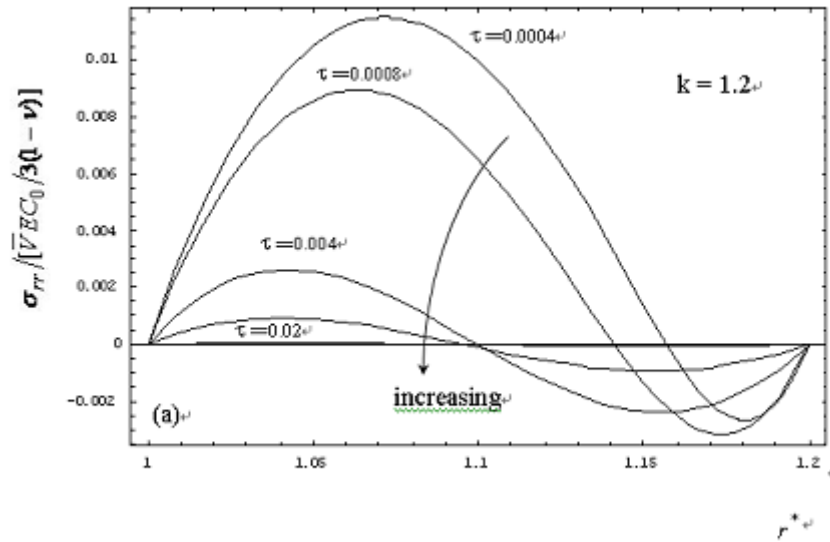


Fig.1 (a)

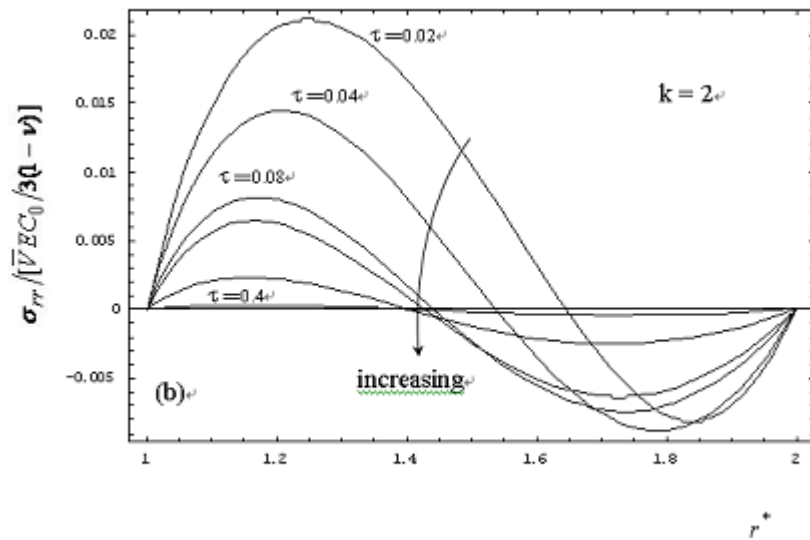


Fig.1 (b)

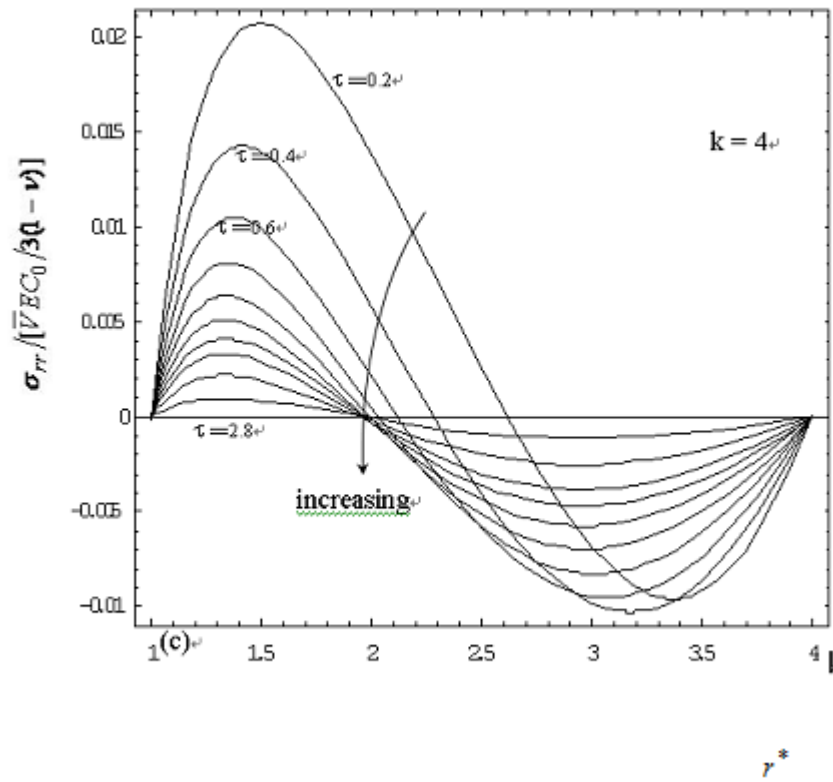


Fig.1 (c)

Fig. 1 The radial stress of with various diffusion times for case A. (a) $k = 1.2$ (b) $k = 2$ (c) $k = 4$.

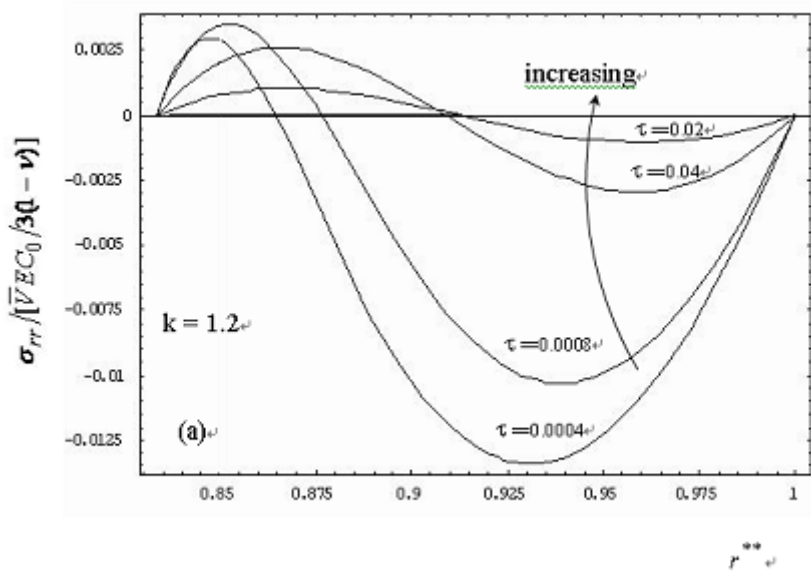


Fig.2 (a)

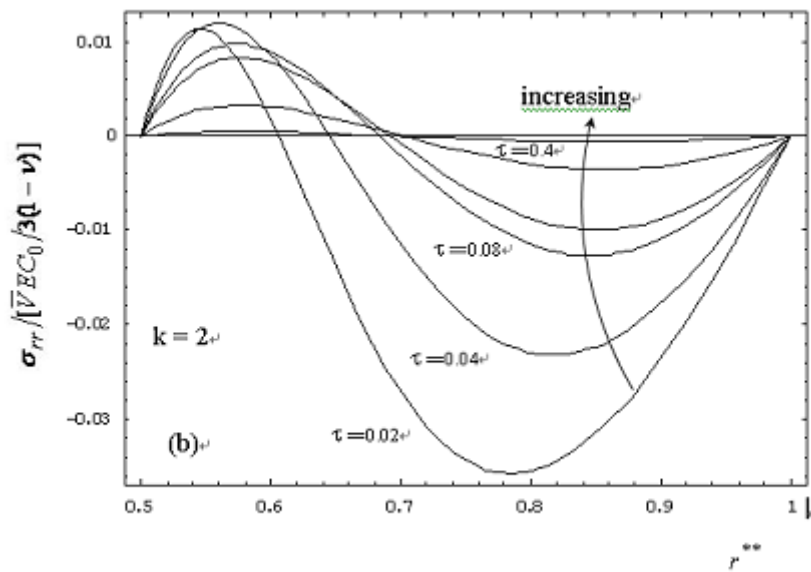


Fig.2 (b)

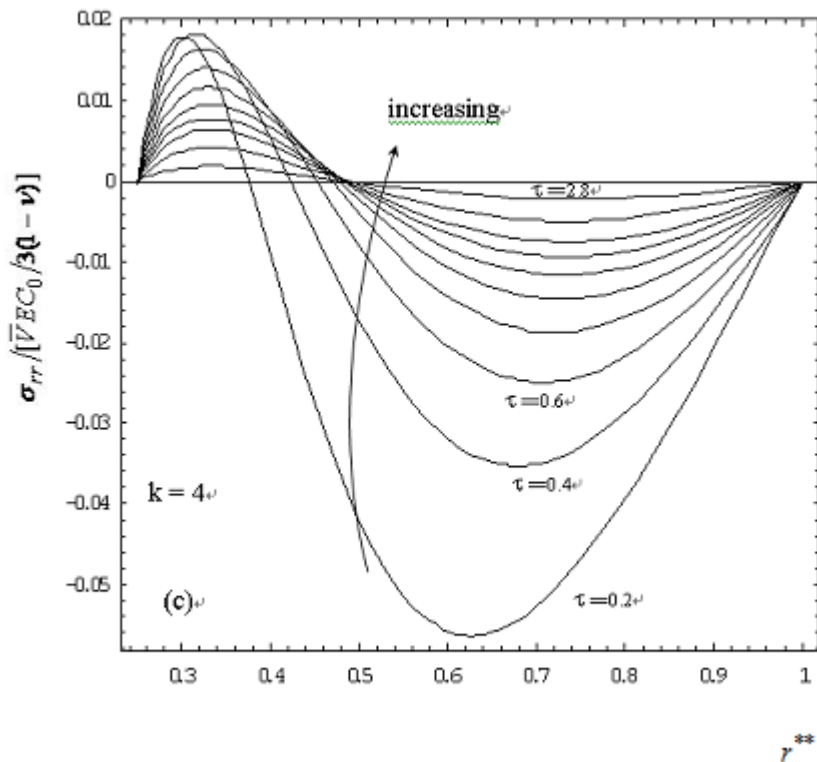


Fig.2 (c)

Fig. 2 The radial stress of σ_{rr} with various diffusion times for case B. (a) $k = 1.2$ (b) $k = 2$ (c) $k = 4$.

3.2. Tangential stresses

For cases A and B, some values of $\sigma_{\theta\theta}/[\sqrt{V}E C_0/3(1-\nu)]$ predicted by Eqs. (14) and (18) are plotted against r^* and r^{**} for $k = 1.2, 2$ and 4 , at various time as shown in Figs. 3 (a)-(c) and Figs. 4 (a)-(c), respectively. As shown in Figs. 3, the tangential stress component $\sigma_{\theta\theta}$ is tensile in the region near both surfaces and compressive in the middle region of hollow cylinder. The stress distribution decreases with increasing time. The curves of $\sigma_{\theta\theta}$ are similar to parabolic curves. It is found that the slope of the curve near the outer surfaces is steeper in the brief times for $k = 1.2$. However, the slope of the curve

near the inner surfaces is constant. For case B, the tangential stress has the same situation as that in case A as shown in the Figs.4.

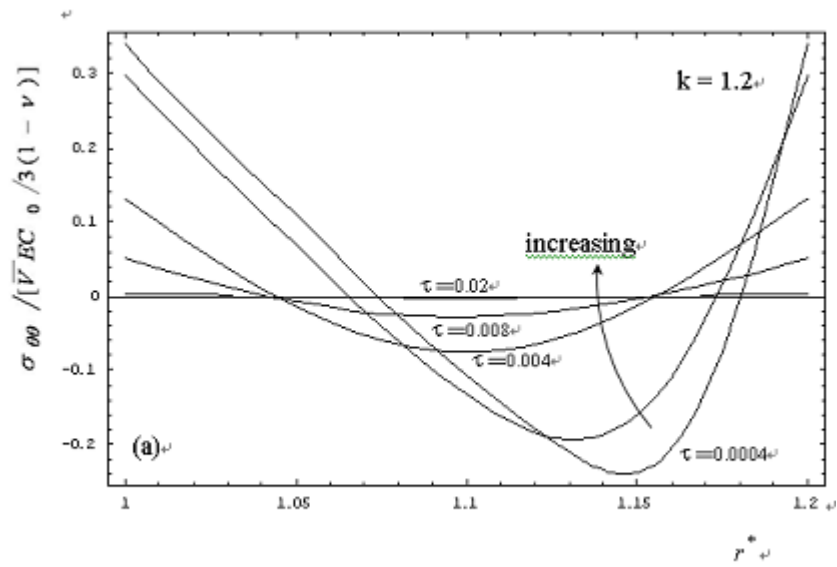


Fig.3 (a)

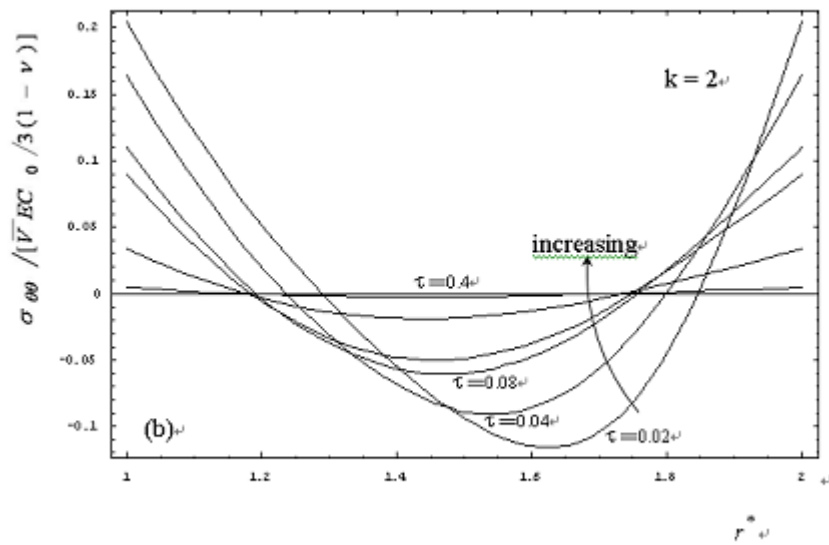


Fig.3 (b)

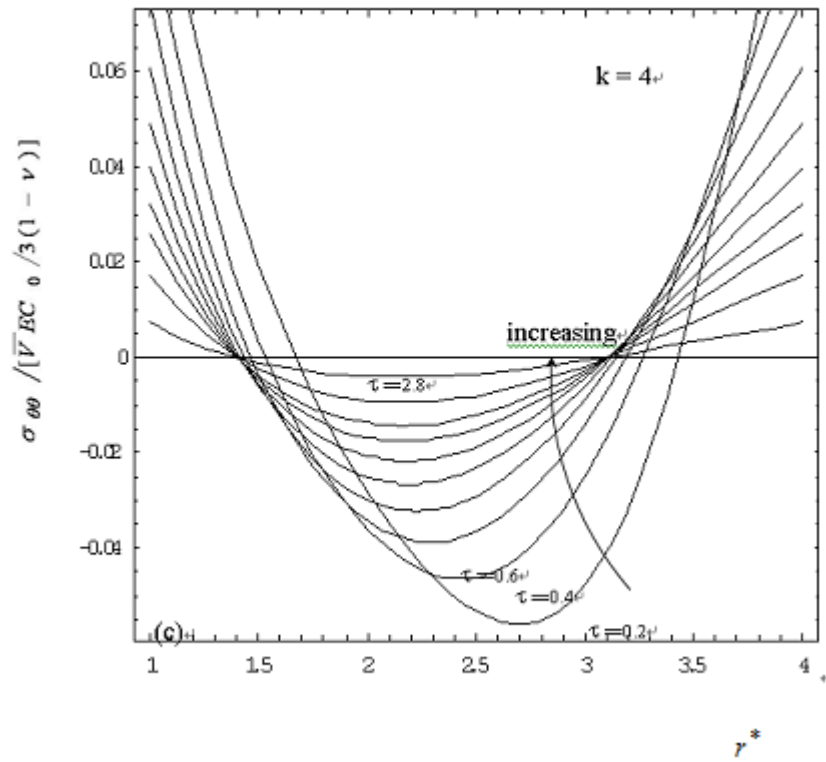


Fig.3 (c)

Fig. 3 The tangential stress of with various diffusion times for case A. for (a) $k = 1.2$ (b) $k = 2$ (c) $k = 4$.

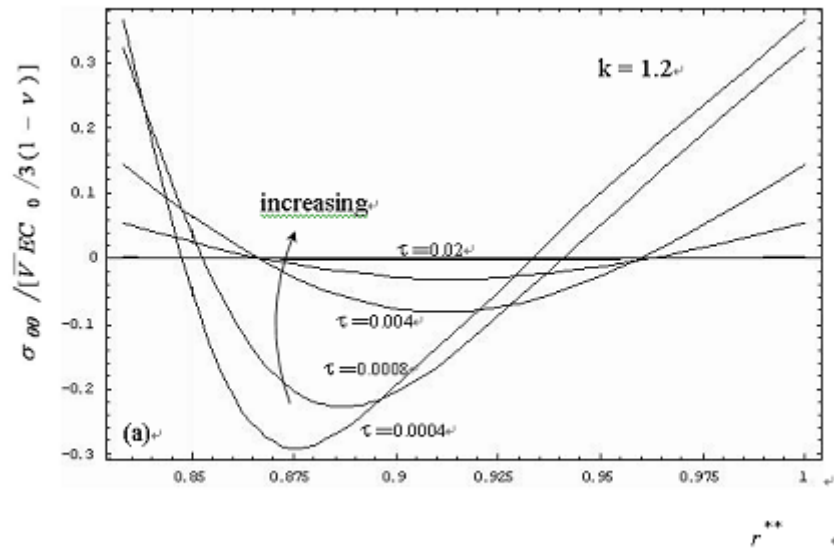


Fig.4 (a)

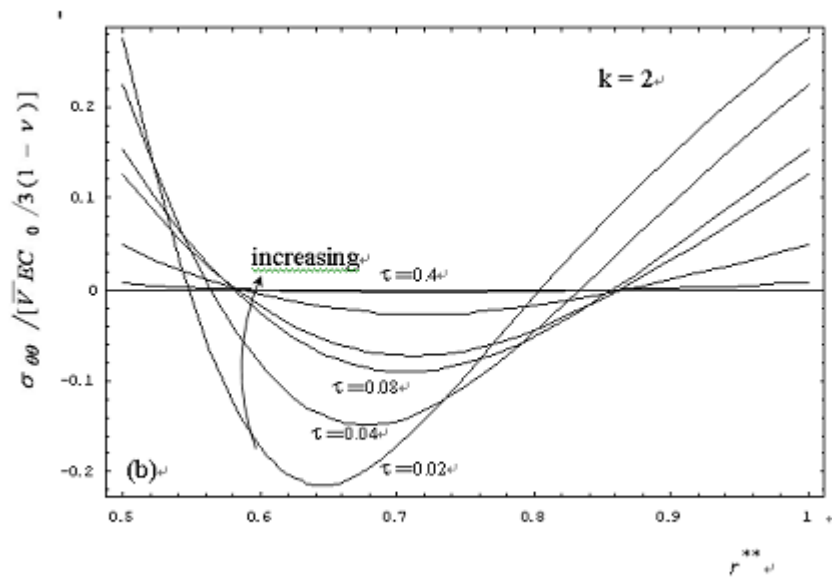


Fig.4 (b)

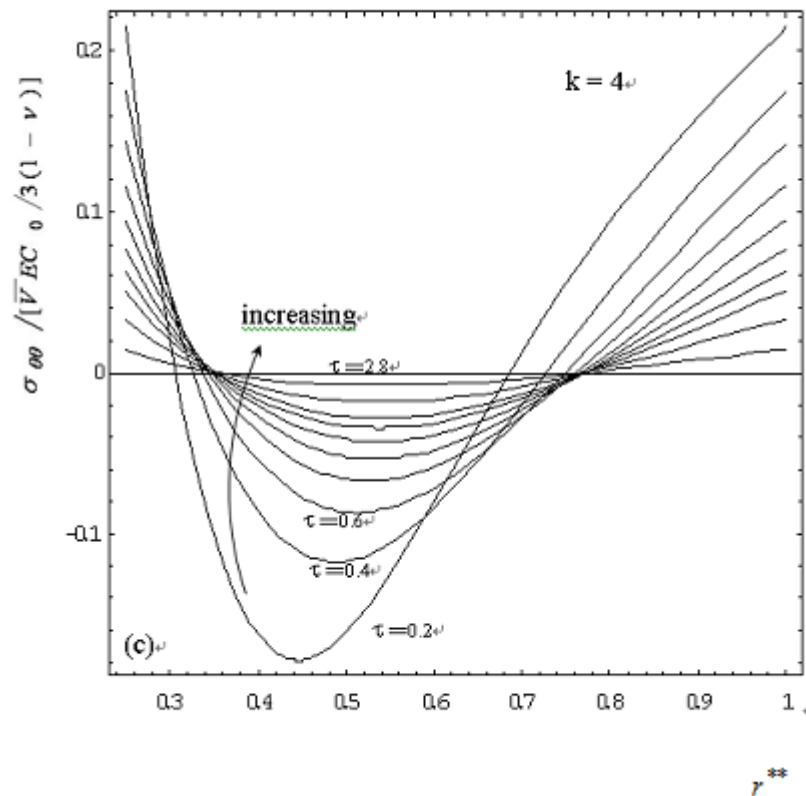


Fig.4 (c)

Fig. 4 The tangential stress of $\sigma_{\theta\theta}$ with various diffusion times for case B. (a) $k = 1.2$ (b) $k = 2$ (c) $k = 4$.

3.3. Axial stresses

For cases A and B, some values of $\sigma_{zz}/[VE C_0/3(1-V)]$ predicted by Eqs. (15) and (19) are plotted against r^* and r^{**} for $k = 1.2, 2$ and 4 , at various time as shown in Figs. 5 (a)-(c) and Figs. 6 (a)-(c), respectively. As shown in Figs. 5, the axial stress component σ_{zz} is tensile in the region near both surfaces and compressive in the middle region of hollow cylinder. The

axial stresses decreases with increasing time. The profiles of stress component σ_{zz} for zero axial force are similar to those of $\sigma_{\theta\theta}$ because $\sigma_{zz} = \sigma_{rr} + \sigma_{\theta\theta}$ and the value of σ_{rr} is smaller than the value of $\sigma_{\theta\theta}$ by a factor of 30 as shown in Figs. 6.

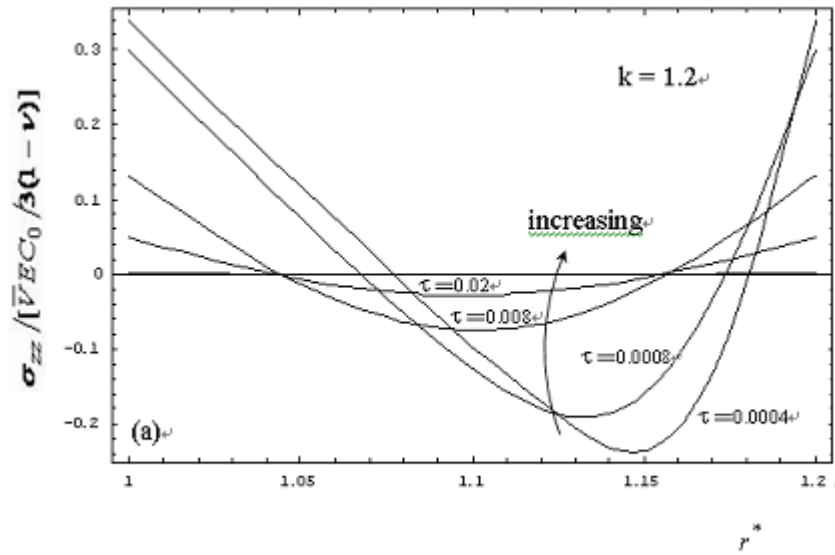


Fig.5 (a)

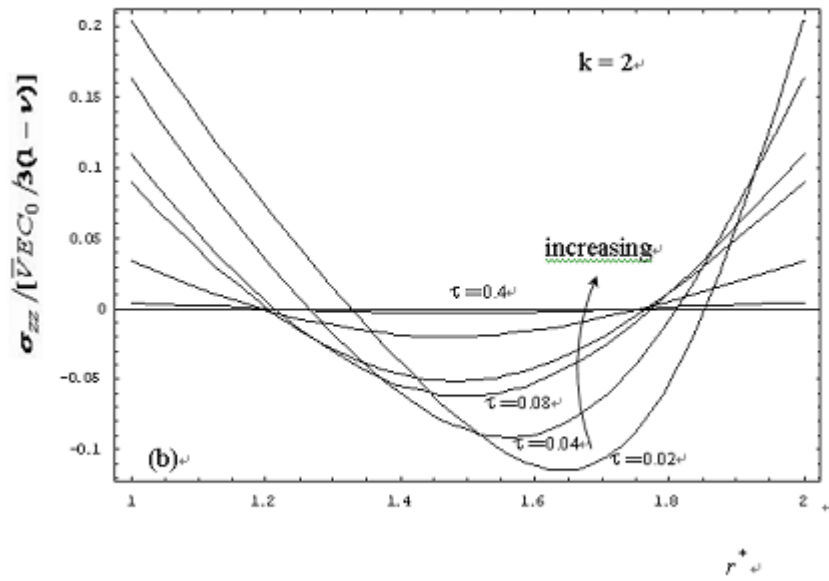


Fig.5 (b)

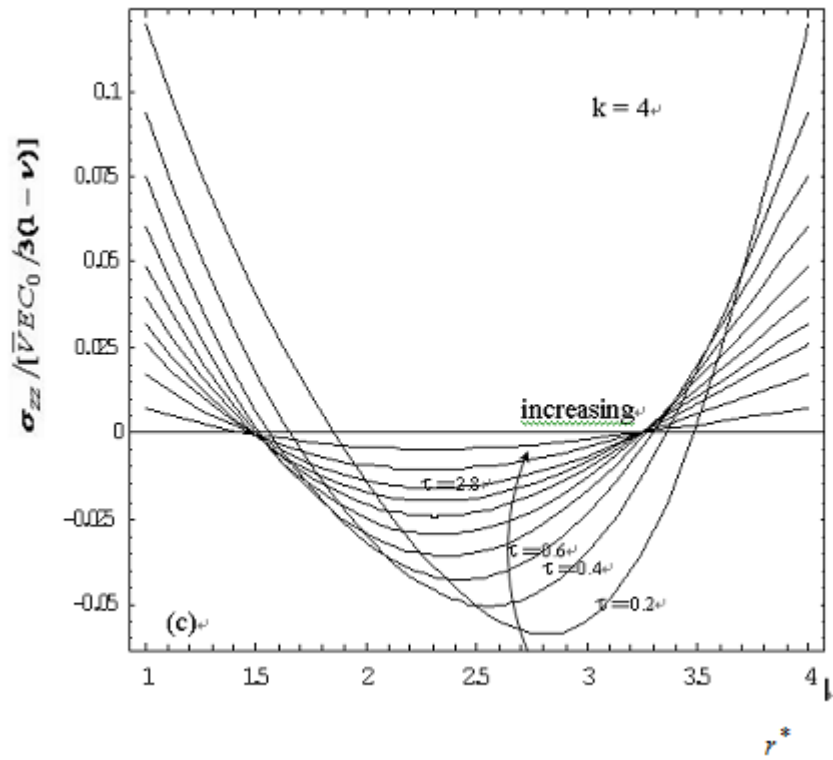


Fig.5 (c)

Fig. 5 The axial stress of with various diffusion times for case A. (a) $k = 1.2$ (b) $k = 2$ (c) $k = 4$.

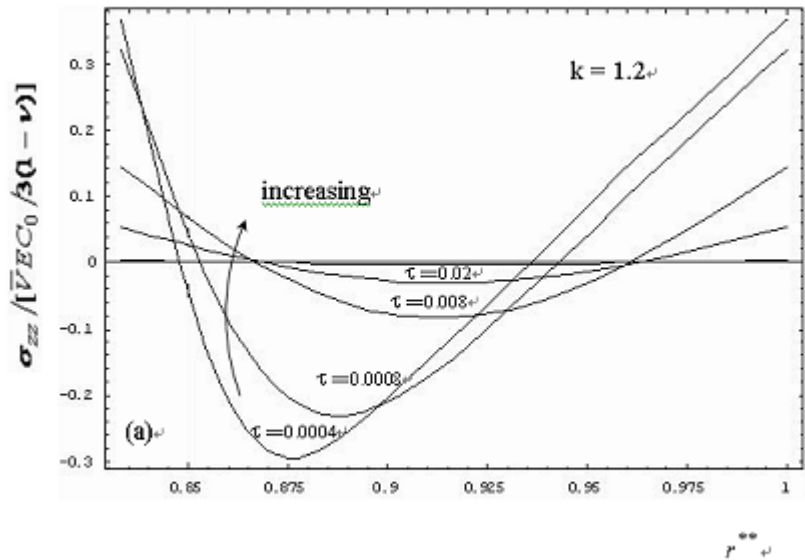


Fig.6 (a)

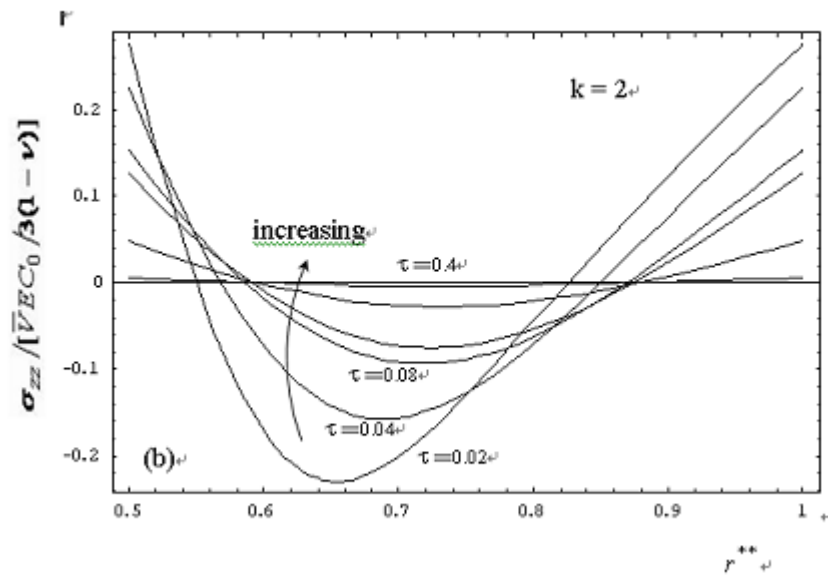


Fig.6 (b)

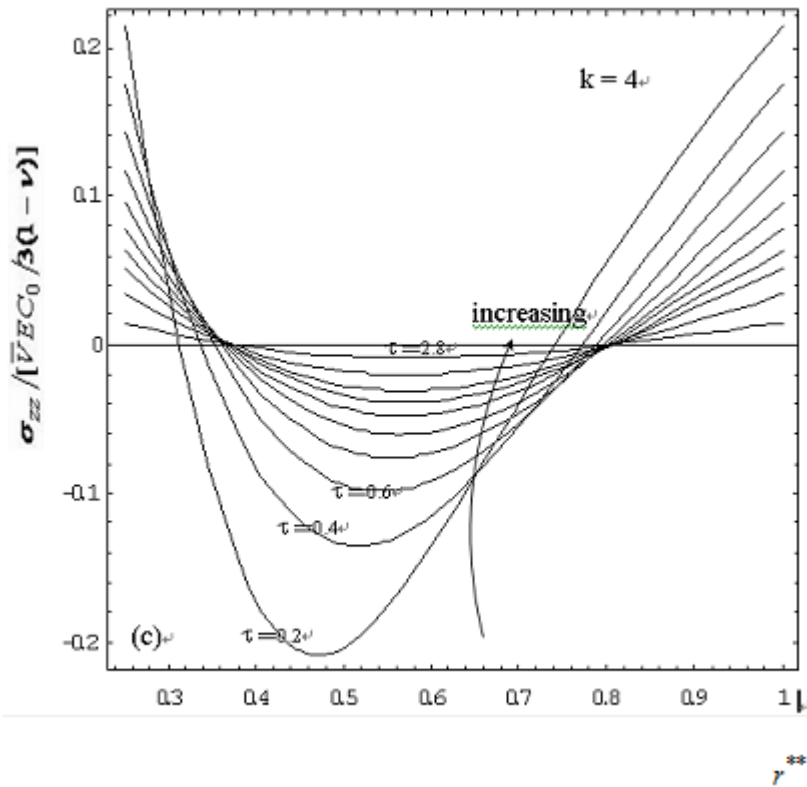


Fig. 6(c)

Fig. 6 The axial stress of with various diffusion times for case B. (a) k=1.2 (b) k= 2 (c) k= 4.

3.4. Maximum shear stresses

Because only the principal stresses exist in the diffusion processes and according to the Mohr's circle constructions [13], the maximum shear stress are

$$(\sigma_{\theta\theta} - \sigma_{rr})/2 (= \sigma_{r\theta}), (\sigma_{zz} - \sigma_{rr})/2 \text{ and } (\sigma_{zz} - \sigma_{\theta\theta})/2.$$

For zero axial force,

$$\sigma_{zz} - \sigma_{rr} = \sigma_{\theta\theta}, \quad \sigma_{zz} - \sigma_{\theta\theta} = \sigma_{rr} \quad \text{and} \quad \sigma_{rr}, \quad \sigma_{\theta\theta}$$

are shown in Figs. 1- 4 for case A and B respectively.

For cases A and B, the maximum shear stress component $\sigma_{r\theta}$ can be expressed in the following.

For case A:

$$\begin{aligned} \frac{(\sigma_{\theta\theta} - \sigma_{rr})/2}{\frac{\sqrt{EC_0}}{3(1-\nu)}} &= \left\{ \frac{1}{k^2 - 1} \sum_{n=1}^{\infty} \frac{2J_0^2(k\alpha_n)}{(\alpha_n r^*)^2 J_0(\alpha_n) [J_0(\alpha_n) + J_0(k\alpha_n)]} \right. \\ &\quad \left. \pi \sum_{n=1}^{\infty} \frac{J_0^2(k\alpha_n) [J_0(k\alpha_n) Y_1(\alpha_n r^*) - Y_0(k\alpha_n) J_1(\alpha_n r^*)]}{\alpha_n r^* [J_0^2(\alpha_n) - J_0^2(k\alpha_n)]} \right. \\ &\quad \left. \sum_{n=1}^{\infty} \frac{2J_0^3(k\alpha_n)}{(\alpha_n r^*)^2 J_0(\alpha_n) [J_0^2(\alpha_n) - J_0^2(k\alpha_n)]} - \frac{\pi}{2} \sum_{n=1}^{\infty} \frac{J_0^2(k\alpha_n) U_0(\alpha_n r^*)}{J_0^2(\alpha_n) - J_0^2(k\alpha_n)} \right\} \\ &\quad \times \exp[-(\alpha_n)^2 \tau] \end{aligned} \quad (20)$$

Where

$$U_0(\alpha_n r^*) = J_0(\alpha_n r^*) Y_0(k\alpha_n) - Y_0(\alpha_n r^*) J_0(k\alpha_n)$$

$$r^* = \frac{r}{a} \quad k = \frac{b}{a} \quad \tau = \frac{Dt}{a^2}$$

For case B:

$$\begin{aligned} \frac{(\sigma_{\theta\theta} - \sigma_{rr})/2}{\frac{\sqrt{EC_0}}{3(1-\nu)}} &= \left\{ -\frac{1}{k^2 - 1} \sum_{n=1}^{\infty} \frac{2J_0(k\alpha_n)}{(k\alpha_n r^{**})^2 [J_0(\alpha_n) + J_0(k\alpha_n)]} \right. \\ &\quad \left. \pi \sum_{n=1}^{\infty} \frac{J_0(\alpha_n) J_0(k\alpha_n) [J_0(k\alpha_n) Y_1(k\alpha_n r^{**}) - Y_0(k\alpha_n) J_1(k\alpha_n r^{**})]}{k\alpha_n r^{**} [J_0^2(\alpha_n) - J_0^2(k\alpha_n)]} \right. \\ &\quad \left. \sum_{n=1}^{\infty} \frac{2J_0^2(k\alpha_n)}{(k\alpha_n r^{**})^2 [J_0^2(\alpha_n) - J_0^2(k\alpha_n)]} + \frac{\pi}{2} \sum_{n=1}^{\infty} \frac{J_0(\alpha_n) J_0(k\alpha_n) U_0(k\alpha_n r^{**})}{J_0^2(\alpha_n) - J_0^2(k\alpha_n)} \right\} \\ &\quad \times \exp[-(\alpha_n)^2 \tau] \end{aligned} \quad (21)$$

where

$$U_0(k\alpha_n r^{**}) = J_0(k\alpha_n r^{**}) Y_0(\alpha_n) - J_0(\alpha_n) Y_0(k\alpha_n r^{**})$$

$$r^{**} = \frac{r}{b} \quad k = \frac{b}{a} \quad \tau = \frac{Dt}{a^2}$$

According to Eqs. (20) and (21), for cases A and B, the maximum shear stress component $(\sigma_{\theta\theta} - \sigma_{rr})/2 = \sigma_{r\theta}$, are plotted against r and r^* for $k = 1.2, 2$ and 4 , at various time as shown in Figs. 7 (a)-(c) and Figs. 8 (a)-(c), respectively.

As shown in Figs. 7, for case A, the maximum shear stress component $\sigma_{r\theta}$ is tensile in the region near both surfaces and compressive in the middle region of hollow cylinder. The stress distribution decreases with increasing time. For case B, the maximum shear stress has the same situation as that in case A as shown in Figs. 8. Comparison of the maximum shear stress in cases A and B, case B is larger, for the same k during the decay transient state. The curves of $\sigma_{r\theta}$ are similar to parabolic curves for $k = 2$ (see Fig. 7 (b)). For case A, it is found that the slope of curve near the outer surface is steeper in the brief times, but the slope of curve near the inner surface is constant for $k = 1.2$. Conversely, for case B, the slope of curve near the inner surface is steeper in the brief times, but the slope of curve near the outer surface is constant.

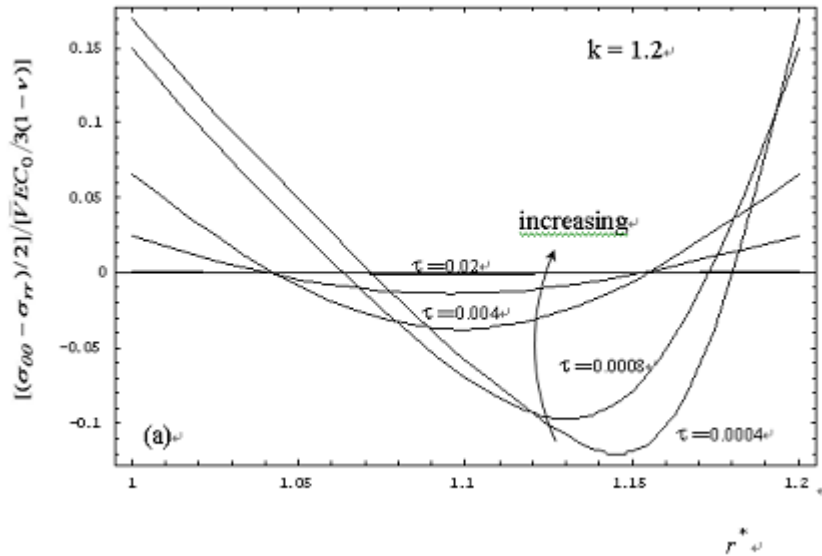


Fig. 7 (a)

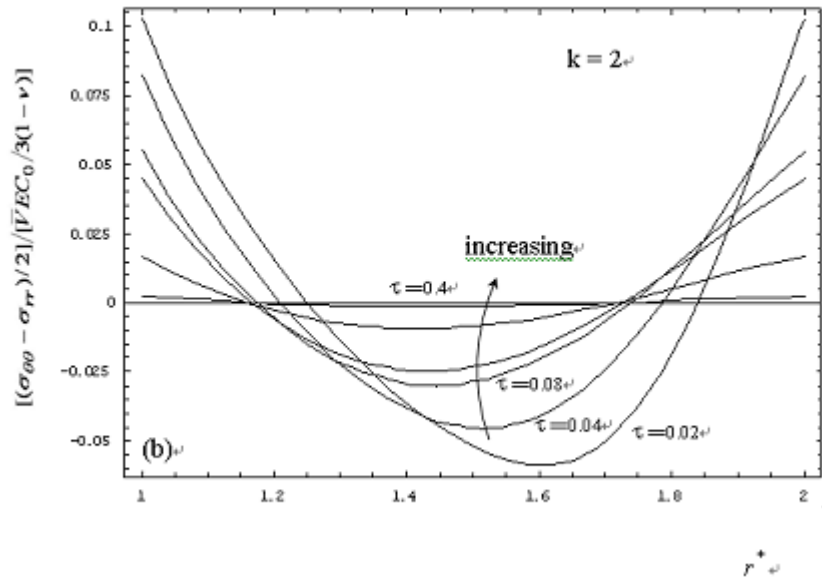


Fig. 7 (b)

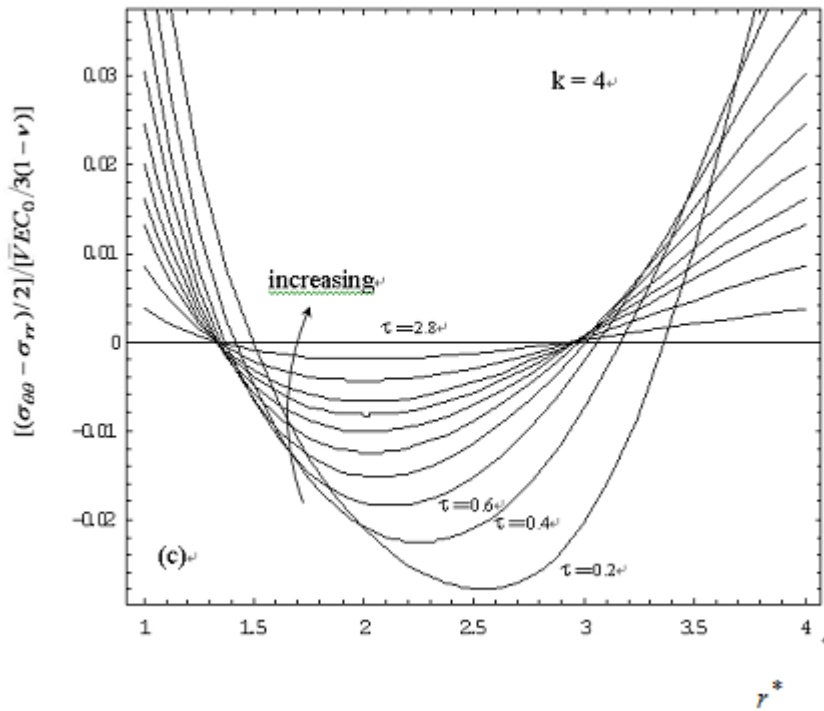


Fig. 7 (c)

Fig. 7 The maximum shear stress of with various diffusion times for case A. (a) $k=1.2$ (b) $k=2$ (c) $k=4$.

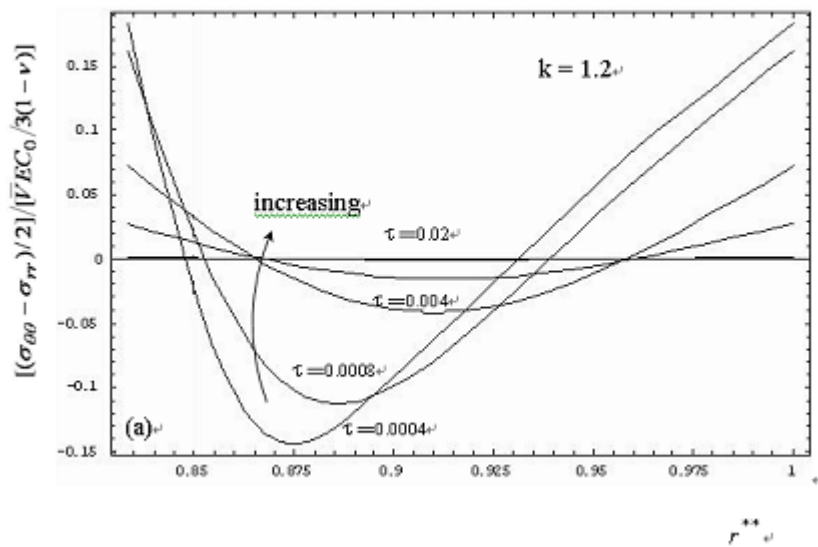


Fig. 8 (a)

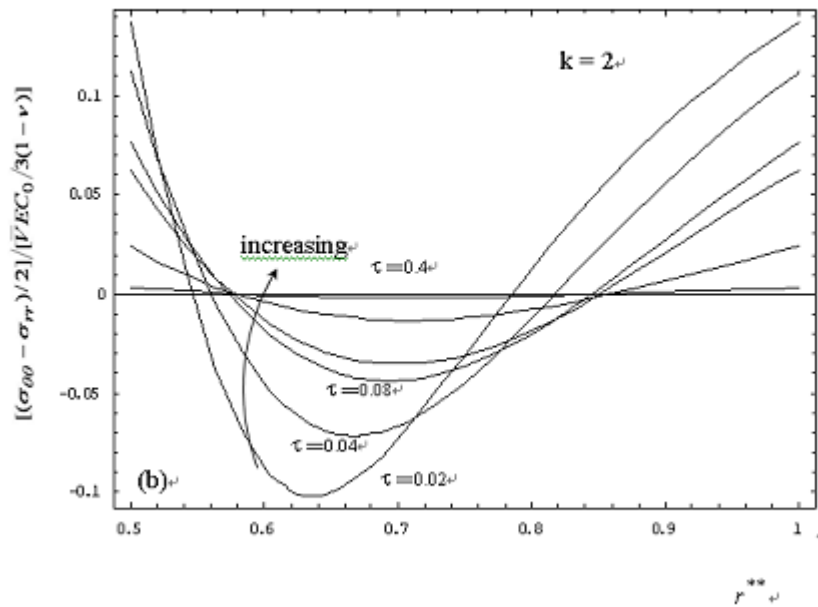
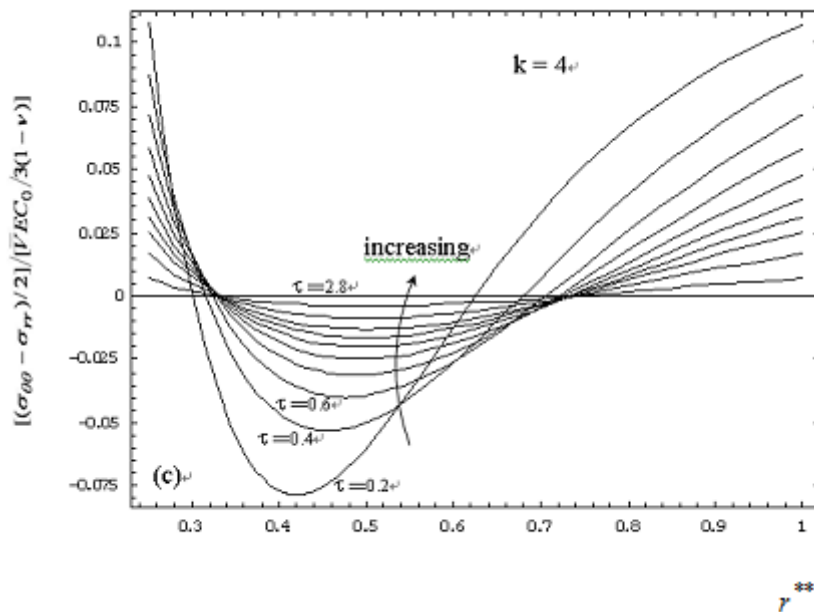


Fig. 8 (b)



Figs. 8 (c)

Fig. 8 The maximum shear stress of τ with various diffusion times for case B. (a) $k=1.2$ (b) $k=2$ (c) $k=4$.

IV. CONCLUSIONS

The diffusion-induced stress in hollow cylinders with different k for decay transient states has been investigated. Two situations are considered: one is a diffusion process, with the initial concentration described by $C=C_0 \ln(r/a)/\ln(b/a)$, in which the solute diffuses from outer into inner surfaces when steady state has finished and zero concentrations at both boundary surfaces and the other with the initial concentration described by

$C=-C_0 \ln(r/b)/\ln(b/a)$, in which the solute diffuses from inner into outer surfaces when steady state has finished and zero concentrations at both boundary surfaces were studied. Analogues to thermal stresses, the diffusion-induced stress developed in hollow cylinders for decay transient states are derived for zero axial force. Through the mathematical analysis and figures plotting, a few conclusions are drawn:

1. For both cases A and B, the radial stress component σ_r is tensile in the region near the inner surface and compressive near the outer surface. The curves of σ_r are similar to sine curves and for the greater k the more τ is needed to reduce the radial stresses.
2. For cases A and B, the tangential stress component $\sigma_{\theta\theta}$ and the axial stress component σ_{zz} are tensile in the region near both surfaces and compressive in the middle region of hollow cylinder. The profiles of σ_{zz} stress component for zero axial force are similar to those of $\sigma_{\theta\theta}$.
3. For both cases A and B, comparison of the maximum shear stress in cases A and B, case B is larger, for the same k .

REFERENCES

- [1]. S. Prussin, "Generation and Distribution of Dislocations by Solute Diffusion", *Journal of Applied Physics*, vol.32, pp.1876-1881,1961.
- [2]. J. C. M. Li "Physical Chemistry of Some Microstructural Phenomena, " *Metallurgical Transactions A* Vol.9A, pp.1353-1380,1978.
- [3]. R. E. Reed-Hill, *Physical Metallurgy Principles*, second ed., Van Nostrand, New York, 360.1973
- [4]. S. Lee, J. C. M. Li, "Dislocation-free diffusion processes", *Journal of Applied Physics*, Vol.52, pp. 1336-1346,1981.
- [5]. S. Lee, H. Ouyang, "General solution of diffusion-induced stresses ", *Journal of Thermal Stresses*, Vol. 10, pp. 269-282,1987.
- [6]. J. L. Chu, S. Lee, "Diffusion-induced stresses in a long bar of square cross section ", *Journal of Applied Physics*, Vol.73 pp. 3211-3219,1993.
- [7]. J. L. Chu, S. Lee, "Chemical stresses in composite circular cylinders", *Journal of Applied Physics*, Vol.73, pp.2239-2248,1993.
- [8]. S. Lee, W. L. Wang, J. R. Chen, "Diffusion-induced stresses in a hollow cylinder: Constant surface stresses", *Materials Chemistry and Physics*, Vol.64, pp. 123-130,2000.
- [9]. S. Lee, W. L. Wang, J. R. Chen, "Diffusion-induced stresses in a hollow cylinder", *Materials Science and Engineering A*, Vol.285, pp.186-194,2000.
- [10]. H. S. Carslaw, J. C. Jaeger, *Conduction of Heat in Solids*, Clarendon Press, Oxford, 1959, 205-207.
- [11]. I. B. Huang, S. K. Yen, "Diffusion in hollow cylinders for some boundary conditions I. Mathematical treatment", *Materials Chemistry and Physics*, Vol. 74, pp.289-299, 2002.
- [12]. S. P. Timoshenko, J. N. Goodier, *Theory of Elasticity*, third ed., McGraw-Hill, New York, 1970, chapter 13.
- [13]. G. E. Dieter, *Mechanical Metallurgy*, second ed., McGraw-Hill, New York, 1976, chapters 2 and 3.